Supporting Information

Rational design of α-helix stabilized Exendin-4 analogues

Near-UV ECD measurements

The near-UV spectrum reports on the ^1L_b band of Tyr as well as on the ^1L_a and ^1L_b overlapping broad bands of Trp (Figure S1). The near-UV ECD spectrum of E0 shows a smaller contribution of the Tyr side-chain ($\sim$ 275 nm) and the ^1L_b band of Trp ($\sim$ 291 nm) than the near-UV ECD spectra of E5 or E10, suggesting partial buried or non-interacting aromatic side-chains. The increasing intensity of the ^1L_a and ^1L_b bands signals the burial of the aromatic side-chains which confirms that the Tyr^{22} and Trp^{25} side-chains are buried in the folded state while solvent exposed in the unfolded states.

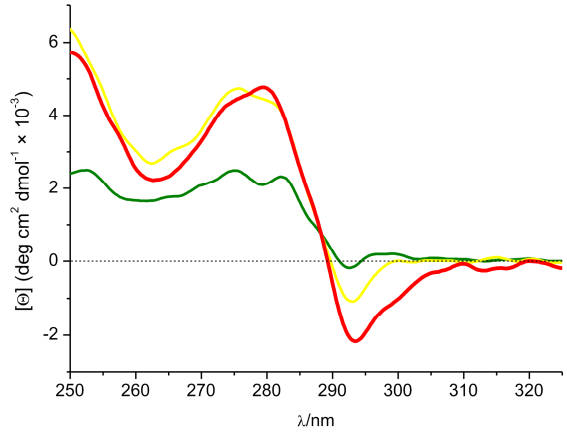

Figure S1: Near-UV ECD spectra of E0 (olive), E5 (yellow) and E10 (red) in water at 5 °C, pH: 6.5 – 7.0.

Calculation of Chemical Shift Deviations

Hα chemical shifts are inherently sensitive to the local chemical environment, particularly to the secondary structure formation. Significantly upfielded Hα proton chemical shifts indicate α-helix formation, while downfielded Hα resonances (positive with respect to the random coil values) are associated with β-sheet preference. Transiently or not fully formed secondary structures can be identified by evaluating the chemical shift deviation (CSD), also known as secondary chemical shift, where CSD $= \delta_{\text{obs}} - \delta_{\text{rc}}$ and δ_{obs} is the observed chemical shift referenced to DSS and δ_{rc} is the random coil chemical shift.

Trp-cage miniproteins exhibit large chemical shift deviations due to the ring-current effect of the indole ring of the central Trp residue and moderate CSDs due to the dipole field of the $L^{21} - D^{28}$ α-helix. The sign and relative magnitude of these chemical shifts deviations are remarkably consistent throughout the Trp-cage variants. Therefore it is feasible to estimate the relative stability of the constructs based on the absolute magnitude of the chemical shift deviations. In the present work, we employ the sum of certain CSDs (CSD_{cage} and $\text{CSD}_{\text{helix}}$) to measure the fraction of the folded and unfolded states (χ_{F} and χ_{U}) as introduced Barua et al. (*52*). CSD_{cage} is derived from the sum of the absolute CSD values of the following eight protons: $L^{26}H\alpha$, $G^{30}H\alpha2$, $P^{31}H\beta2$, $R^{35}H\alpha$, $P^{37}H\alpha$, $P^{37}H\beta2$, $P^{39}H\delta1$ and $P^{38}H\delta2$, all experiencing the magnetic environment of the indole ring. We also incorporated $W^{25}N\epsilon1$ CSD in the calculation of CSD_{cage} since it forms a crucial structure stabilizing H-bond with the carbonyl of R^{35} (or G^{34}) which greatly affects its chemical shift ($\delta_{\text{H}\epsilon1}$ shifts upfield upon H-bond formation). $\text{CSD}_{\text{helix}}$ is calculated from the CSD of four Hα protons of the α-helix: $Y^{22}H\alpha$, $Q^{24}H\alpha$, $W^{25}H\alpha$ and $K^{27}H\alpha$.

Folded and unfolded fractions (χ_{F} and $\chi_{\text{U}} = 1 - \chi_{\text{F}}$) were derived from the CSD values assuming a linear correlation between the observed CSD and the amount of molecules in the folded state. For the calculations we used both folded and unfolded baselines: a disulfide-bridge stabilized E5 variant, E5_A4C_S25C was used as folded reference ($\chi_{\text{F}} = 1$) while a variant phosphorylated at the C-terminal serine position (Tc5b_S20pS) was selected

as unfolded reference with an assumed 5% folded population. The baseline chemical shift references were assumed to be temperature independent. In this model we assume that all investigated variants can be described with the same Trp-cage structure (differing only at the length of its α-helix) and all observed differences in any spectral properties are the consequence of the shift in populations. As the fold is destabilized (e.g., with the N20R mutation) χ_U increases and χ_F decreases but the overall folded structure is unaffected.

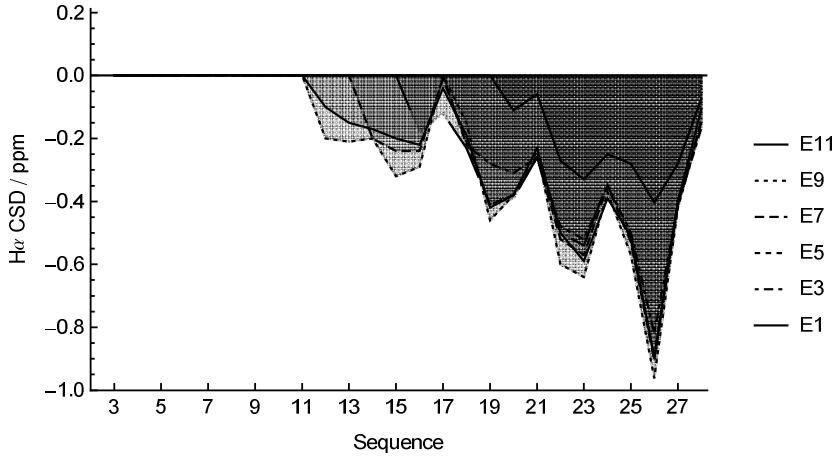

Figure S2: Hα chemical shift deviations of E11, E9, E7, E5, E3 and E1 in the $Glu^3 - Glu^{28}$ segment.

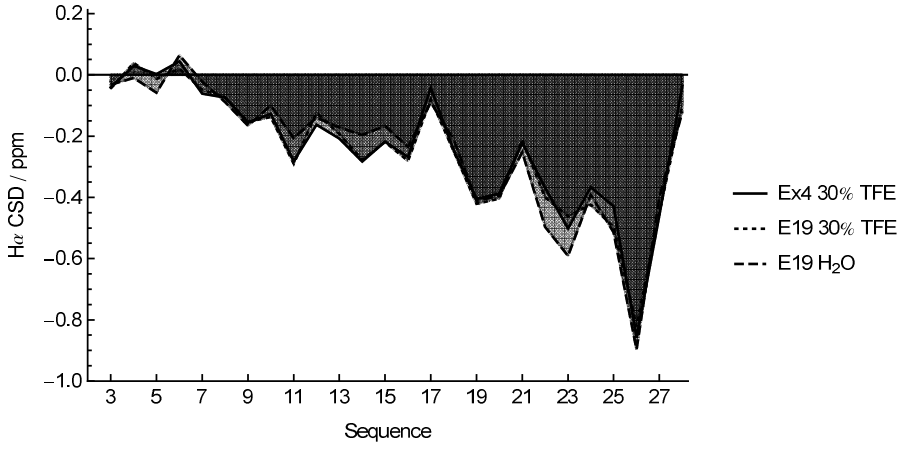

Figure S3: Hα chemical shift deviations of E19 and Ex4 in the $Glu^3 - Glu^{28}$ / Asn^{28} segment.

Table S1: Chemical shift deviations of the N-terminal elongated Trp-cage variants

			Chemical shift deviation												
Name	**Sequence**	T/°C	26α	30α2	31β2	35α	37α	37β2	38δ1	38δ2	25ϵ1	22α	24α	25α	27α
	Random Coil reference chemical shifts		4.23	4.02	2.27	4.62	4.69	2.29	3.74	3.59	10.22	4.60	4.37	4.70	4.36
Ex4 30%TFE	HGEGTFTSDLSKQMEEEAVRLFIEWLKNGGPSSGAPPPS	27	-0.86	-2.66	0.19	0.33	-1.58	-1.35	-0.55	-0.50	-0.46	-0.37	-0.37	-0.43	-0.46
E19 30%TFE	HGEGTFTSDLSKQMEEEAVRLYIQWLKEGGPSSGRPPPS	27	-0.82	-3.11	0.24	0.39	-2.06	-1.79	-0.69	-0.68	-0.48	-0.40	-0.42	-0.50	-0.45
E19	HGEGTFTSDLSKQMEEEAVRLYIQWLKEGGPSSGRPPPS	27	-0.90	-2.98	0.22	0.33	-2.03	-1.77	-0.65	-0.63	-0.58	-0.50	-0.39	-0.51	-0.40
E11	DLSKQMEEEAVRLYIQWLKEGGPSSGRPPPS	27	-0.90	-2.95	0.22	0.34	-2.01	-1.76	-0.63	-0.61	-0.58	-0.50	-0.39	-0.51	-0.40
E11	DLSKQMEEEAVRLYIQWLKEGGPSSGRPPPS	5	-0.91	-3.25	0.24	0.40	-2.20	-1.97	-0.68	-0.64	-0.26	-0.53	-0.36	-0.54	-0.42
E10	LSKQMEEEAVRLYIQWLKEGGPSSGRPPPS	5	-0.96	-3.30	0.24	0.40	-2.30	-2.02	-0.64	-0.68	-0.56	-0.60	-0.37	-0.57	-0.42
E9	SKQMEEEAVRLYIQWLKEGGPSSGRPPPS	5	-0.91	-3.22	0.24	0.40	-2.23	-1.93	-0.65	-0.67	-0.56	-0.51	-0.34	-0.53	-0.40
E8	KQMEEEAVRLYIQWLKEGGPSSGRPPPS	5	-0.91	-3.23	0.24	0.39	-2.23	-1.93	-0.66	-0.69	-0.57	-0.52	-0.35	-0.53	-0.41
E7	QMEEEAVRLYIQWLKEGGPSSGRPPPS	5	-0.91	-3.22	0.24	0.40	-2.23	-1.93	-0.66	-0.68	0.00	-0.52	-0.35	-0.53	-0.40
E6	MEEEAVRLYIQWLKEGGPSSGRPPPS	5	-0.90	-3.20	0.25	0.39	-2.21	-1.93	-0.65	-0.69	-0.57	-0.50	-0.34	-0.52	-0.40
E5	EEEAVRLYIQWLKEGGPSSGRPPPS	5	-0.88	-3.17	0.25	0.35	-2.19	-1.91	-0.63	-0.64	-0.56	-0.48	-0.33	-0.51	-0.40
E4	EEAVRLYIQWLKEGGPSSGRPPPS	5	-0.82	-2.84	0.19	0.30	-1.99	-1.73	-0.60	-0.61	-0.53	-0.48	-0.35	-0.50	-0.41
E3	EAVRLYIQWLKEGGPSSGRPPPS	5	-0.57	-2.06	0.17	0.23	-1.52	-1.59	-0.39	-0.42	-0.36	-0.35	-0.28	-0.36	-0.32
E2	AVRLYIQWLKEGGPSSGRPPPS	5	-0.39	-1.37	0.12	0.14	-0.94	n.d.	-0.23	-0.26	-0.24	-0.27	-0.25	-0.28	-0.29
E1	VRLYIQWLKEGGPSSGRPPPS	5	-0.31	n.d.	0.09	0.11	n.d.	n.d.	-0.18	-0.21	-0.20	-0.24	-0.24	-0.25	-0.28
E0	RLYIQWLKEGGPSSGRPPPS	5	-0.28	-0.85	0.08	0.08	n.d.	n.d.	-0.16	-0.17	-0.17	-0.21	-0.23	-0.22	-0.27
TC	NLYIQWLKEGGPSSGRPPPS	5	-0.80	-2.96	0.24	0.35	-2.06	-1.78	-0.59	-0.59	-0.52	-0.45	-0.33	-0.48	-0.37
TC	NLYIQWLKEGGPSSGRPPPS	27	-0.56	-1.86	0.15	0.15	n.d.	n.d.	-0.39	-0.38	-0.39	-0.33	-0.30	-0.32	-0.30
F ref	EEECVRLYIQWLKDGGPSSGRPPPC	15	-0.82	-3.43	0.27	0.44	-2.49	-1.80	-0.80	-0.83	-0.62	-0.61	-0.46	-0.46	-0.43
U ref	NLYIQWLKDGGPSSGRPPPpS	15	-0.07	-0.07	0.02	-0.03	-0.16	-0.09	-0.01	-0.03	-0.08	-0.11	-0.21	-0.07	-0.19

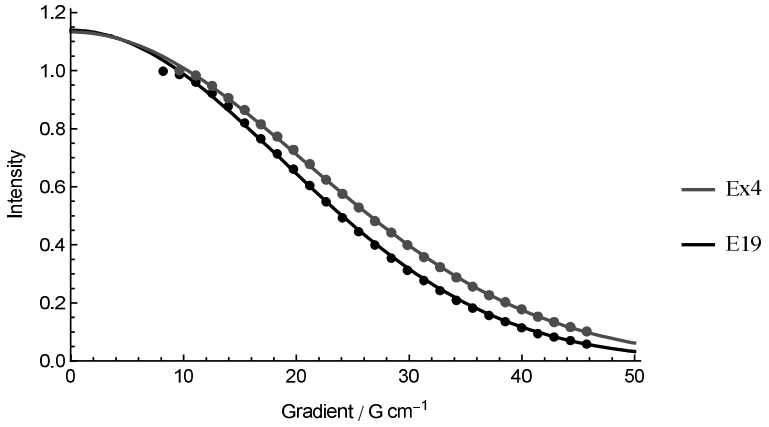

Figure S4: Normalized intensities of a methyl signal in the 1D spectra of Ex4 (gray) and E19 (black) versus the strength of the diffusion encoding gradient measured at 27 °C in 30% TFE/70% H_2O solution. Solid lines represent the result of nonlinear regression to equation $I = I_0 \exp(-\gamma^2 g^2 D \delta^2 (\Delta - \delta/3))$. Fitted diffusion coefficients are 9.54×10^{-11} m^2/s and 9.40×10^{-11} m^2/s for E19 and Ex4, respectively.

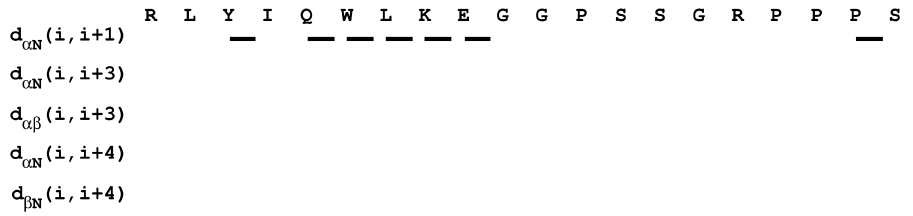

(a) E0

(b) E1

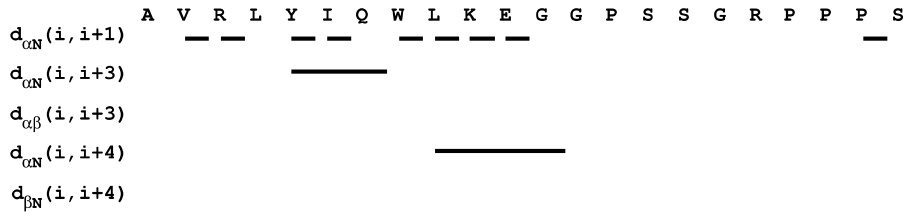

(c) E2

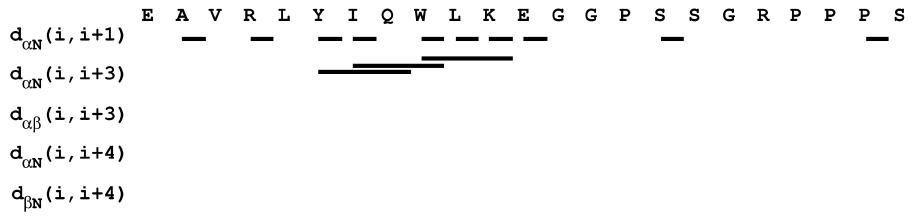

(d) E3

Figure S5: Short and medium range NOE-connectivities of the different elongated variants (E0 − E3).

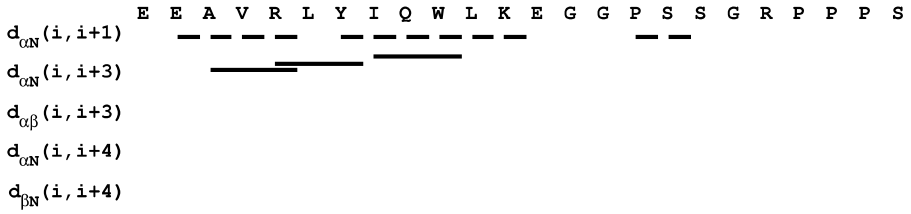

(a) E4

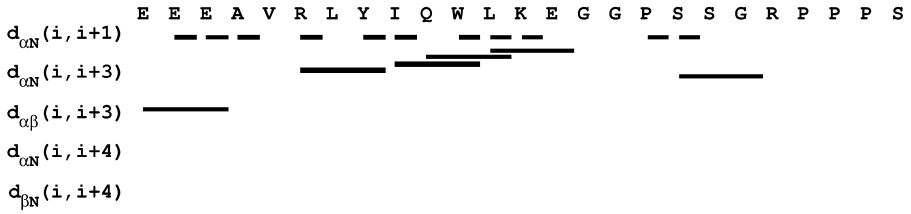

(b) E5

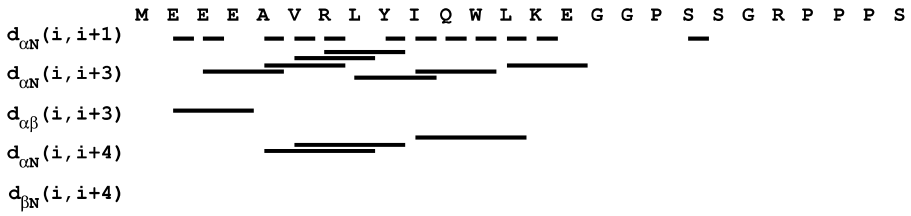

(c) E6

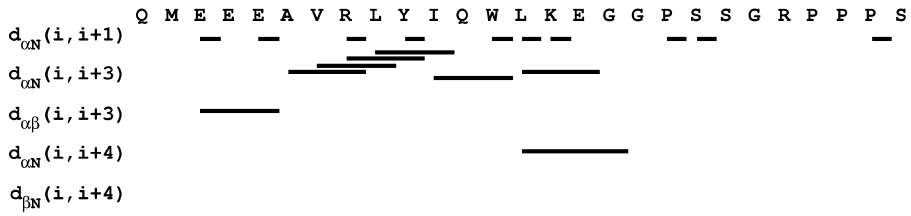

(d) E7

Figure S6: Short and medium range NOE-connectivities of the different elongated variants (E4 − E7).

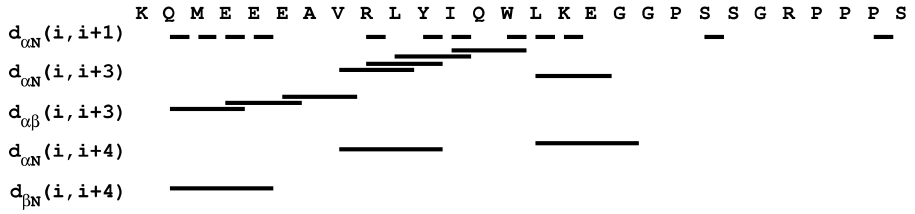

(a) E8

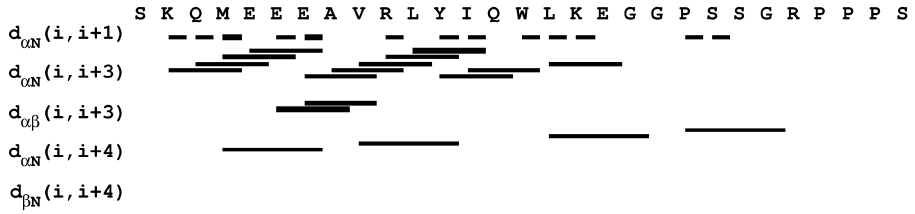

(b) E9

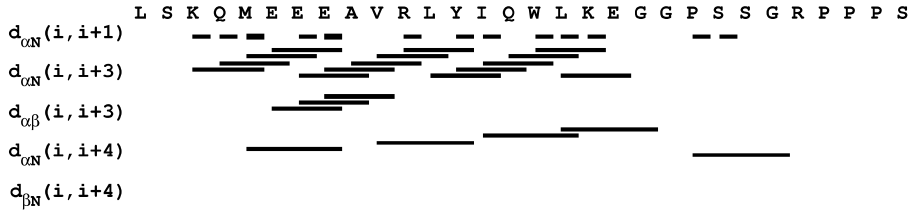

(c) E10

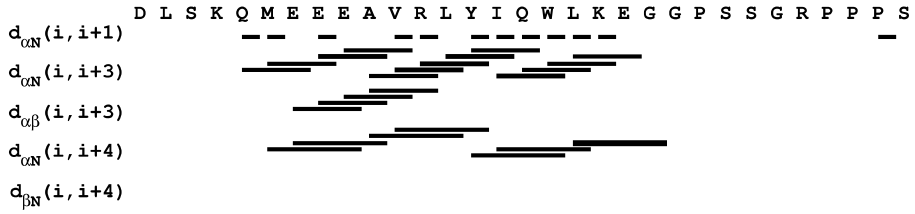

(d) E11

Figure S7: Short and medium range NOE-connectivities of the different elongated variants (E8 − E11).

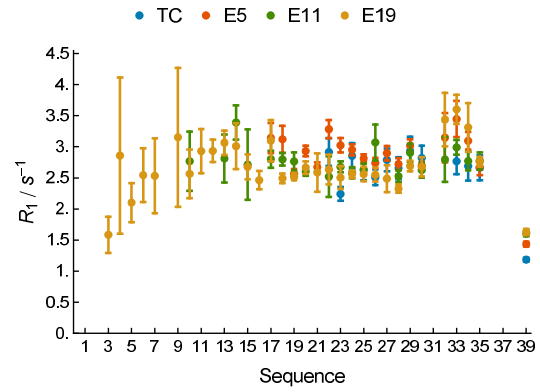

(a)

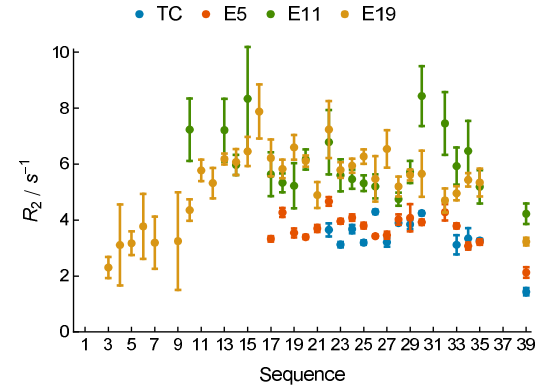

(b)

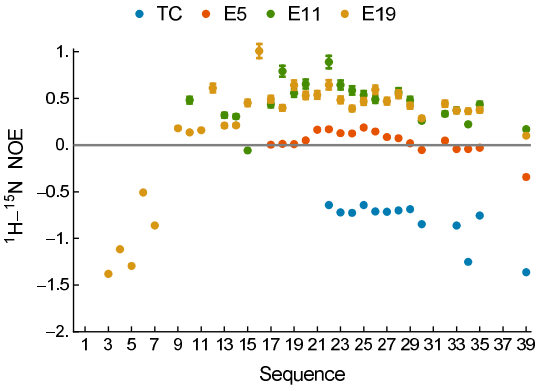

(c)

Figure S8: R_1, R_2 and heteronuclear NOE relaxation parameters of TC, E5, E11, E19 measured at 27 °C at 11.74 T B_0 field strength as a function of residue number.

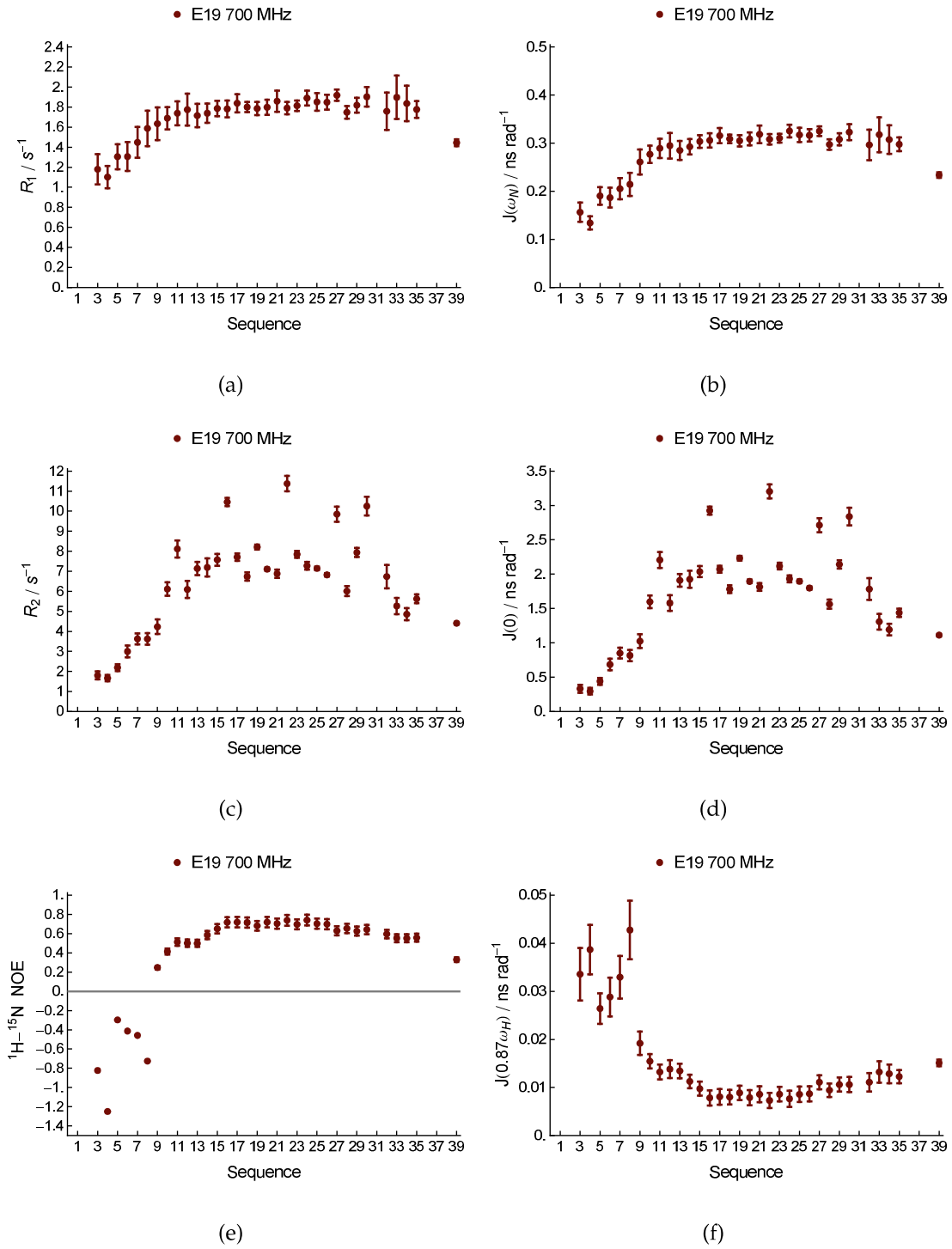

Figure S9: R_1, R_2 and heteronuclear NOE relaxation parameters and $J(0)$, $J(\omega_N)$ and $J(0.87\omega_H)$ spectral density values of E19 measured at 27 °C at 16.4 T B_0 field strength as a function of residue number.